Eur. Phys. J. D **41**, 103–111 (2007)
DOI: 10.1140/epjd/e2006-00200-6

THE EUROPEAN PHYSICAL JOURNAL D

Electron-impact dissociation and transient properties of a stored LiH_2^- beam

L. Lammich[1,a], S. Altevogt[1], H. Buhr[1], H. Kreckel[1], S. Krohn[1], M. Lange[1], D. Strasser[3], R. Repnow[1], M. Grieser[1], R. Schinke[2], Z.-W. Qu[2], H. Zhu[2], D. Schwalm[1], D. Zajfman[3,1], and A. Wolf[1]

[1] Max-Planck Institut für Kernphysik, Heidelberg, Germany
[2] Max-Planck Institut für Strömungsforschung, Göttingen, Germany
[3] Dept. of Particle Physics, Weizmann Institute of Science, Rehovot, Israel

Received 8 June 2006 / Received in final form 7 August 2006
Published online 1st September 2006 –

Abstract. The fragmentation of LiH_2^- anions after electron impact was investigated at the heavy-ion storage ring TSR. The main reaction channel was found to be electron detachment followed by a breakup into LiH + H. In the first ms after production of the molecular ions in a cesium sputtering ion source, additional contributions were observed in the Li + H_2 and Li^- + H_2 channels, hinting at an initial population of a short-lived state of the anion. To gain a better understanding of the mechanisms underlying the observed behavior of the system, ab initio calculations of relevant potential energy surfaces were performed at selected geometries. The experimental findings are discussed in the light of these calculations.

PACS. 34.80.Ht Dissociation and dissociative attachment by electron impact – 34.20.Mq Potential energy surfaces for collisions – 34.50.Gb Electronic excitation and ionization of molecules; intermediate molecular states (including lifetimes, state mixing, etc.)

1 Introduction

The LiH_2^- anion is the most simple stable and covalently bound triatomic negative ion. As in a whole class of metal dihydrides [1], the excess electron stabilizes a compound that is unstable in the neutral state. While a number of theoretical studies have been performed on this prototypical system [1–4], no experimental data on LiH_2^- except for its mass-spectroscopic detection at negative ion sources [5,6] have been reported. In an attempt to record its photoelectron spectrum, no detachment signal was observed using 2.54 eV photons [6]. Aside from the known structure of the covalently bound LiH_2^- molecule [3], another minimum of the anionic ground state potential energy surface (PES) was found in recent calculations, giving rise to the very weakly bound electrostatic complex $Li^-(H_2)$ [4].

The instability of the neutral LiH_2 system makes not only the structure of LiH_2^-, but especially also the electron detachment from the anion an interesting test case, as the dynamics of the subsequent dissociation process are determined by the same PESs which govern the neutral reaction LiH + H ↔ Li + H_2. Because of its fundamental nature and astrophysical importance [7] this chemical reaction is subject to ongoing experimental [8] and theoretical [9,10] studies.

In this paper we present the results of electron-impact fragmentation experiments on LiH_2^- performed in a heavy-ion storage ring, focusing mainly on the investigation of product channels populated in this reaction. Considering the relevant energy levels of the anionic and neutral LiH_2 systems (see Fig. 1), several reactions appear possible: at lower collision energies, a fragmentation might be possible via an electronically excited state of the anion, thus producing neutral and negative fragments. Earlier calculations found such an excited anion state below the lowest neutral state [2], where the autodetachment of an electron is not possible but a fragmentation of the anion might occur, depending on the detailed structure of the PESs involved. However, our new calculations locate this state above the neutral ground state (see Sect. 4).

On the other hand, at higher impact energies, electron detachment is expected to occur with a subsequent dissociation of the neutral system. The vertical ionization potentials (VIPs), which describe the transition energy at the LiH_2^- ground state geometry to the two lowest lying neutral PESs, corresponding to the detachment of a $1\sigma_u$ or a $1\sigma_g$ electron, were calculated to 3.0 eV and 3.35 eV, respectively [1]. While the second neutral surface is geometrically stable at this point, the neutral ground state is instable and the system is expected to dissociate into the

[a] *Present address*: Department of Physics and Astronomy, University of Aarhus, Denmark. e-mail: `lutz@phys.au.dk`

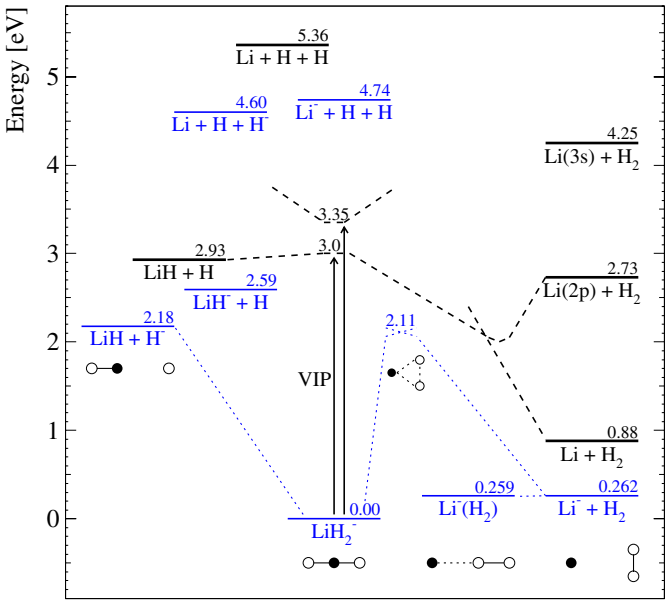

Fig. 1. (Color online) Schematic overview of relevant energy levels assuming the rovibrational ground state for all molecules and infinite separation of unbound fragments, summarizing data from [1,3,4,6,11–13] (VIP = Vertical Ionization Potential). The pictograms visualize the nuclear geometries for some conformations.

$Li + H_2$ channel [1], which is found at an energy of 0.88 eV above the LiH_2^- ground level [3]. The second two-body dissociation channel, LiH + H, has an energy very close to the VIP. It is thus not clear a priori if a fragmentation via this channel is possible. A full fragmentation into Li + H + H (dissociation energy 5.4 eV) could additionally be possible via excitation of high energetic electronic states.

Altogether, an electron impact on LiH_2^- is expected to lead mainly to the $Li + H_2$ dissociative channel. However, taking into account the limited knowledge on the interaction process and the PESs involved, other channels (possibly involving also charged fragments) cannot be excluded.

2 Experimental set-up

The experiment was performed at the TSR heavy ion storage ring [14] located at the Max-Planck-Institut für Kernphysik in Heidelberg, Germany. $^7LiH_2^-$ ions were produced in a cesium sputtering ion source employing a lithium hydride sputtering target, mass selected and accelerated to an energy of 4.5 MeV before being injected into the storage ring. During the storage time of up to 15 s, the ion beam was overlapped in the electron cooling device of the TSR with a co-moving electron beam of adjustable relative energy between the electrons and the molecular ions.

To observe neutral products emerging from ion-electron collisions, a silicon surface barrier detector was used which was mounted straight ahead of the interaction region after the next main bending dipole of the storage ring (see Fig. 2). In addition, a movable scintillator was

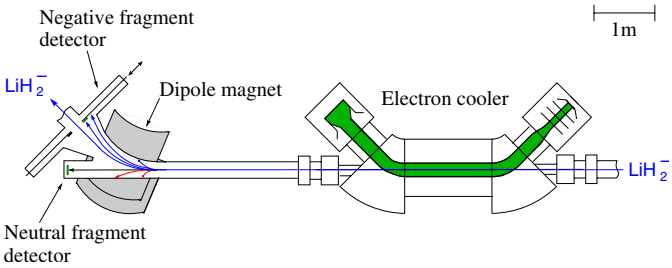

Fig. 2. (Color online) Sketch of the electron cooler at TSR with detectors for charged and neutral reaction products.

employed behind this dipole magnet to detect negative fragments moving close to the orbit of the LiH_2^- beam. This detector was sensitive to LiH^- and Li^- ions, while H^- and positive ions could not be addressed due to the geometry of the set-up.

The energy sensitivity of the solid state detector could be used to determine the total mass of those fragments emerging as neutrals from each single dissociation reaction. In addition, a set of two metal grids was used which could be moved in front of the solid state detector to reduce its efficiency by a well-known factor, thus allowing for a differentiation between the possible chemical compositions of the neutral fragments, see Section 3.2.

To investigate the products of electron-ion collisions at various relative energies, the following timing scheme was applied to the acceleration voltage of the electron beam which controls the relative electron-ion energy E_e. In the first 2 s after ion injection, the electrons were kept at $E_e \approx 0$ eV to allow for rovibrational relaxation before the start of the measurement.

After that, the electron energy was switched in a fast, repeating cycle between three different energies: during the *measurement* step the electron acceleration voltage was set such that a certain detuning energy E_e in the center of mass frame of the moving ions was achieved. This energy was varied from injection to injection to accumulate a complete energy spectrum of the channel-specific impact detachment rates. After this, a fixed *reference* energy was chosen and the count rate observed during this step was used as a measure of the ion beam intensity. Finally, during a *background* step the electron beam was set back to $E_e \approx 0$ eV; as no electron-induced signal is expected at very low collision energies, the signal here could be used to determine the background rate due to residual gas induced fragmentation events, an interpretation that was checked by switching off the electron beam.

Because of the very low ion beam intensity ($\lesssim$ nA) no diagnostic methods were available to ensure a translational cooling of the ion beam. The spread of relative ion-electron collision energies present at a given electron acceleration voltage was thus dominated by the spatial extension of the ion beam in the interaction region. As a space-charge limited electron beam with relative velocity differences of $\sim 10^{-2}$ over its cross-section was used, the spread of collision energies amounts to up to 100 meV in the center of mass frame of the ions. For the experiments

considered here, this uncertainty in the collision energy can be neglected.

Another consequence of the use of an uncooled ion beam is a possible reduction of detection efficiencies. While the solid state detector employed has a ∼100% efficiency for detection of MeV particles, the spatial extension of the ion beam could cause some neutral fragments to miss the detector, thus leading to the detection of a reduced mass, as will be seen below.

3 Results

At storage times larger than a few ms, only neutral fragments were detected following the breakup of LiH_2^-. The results of these measurements are discussed in the following. In the first ms after each ion injection, a different behavior was observed which will be described in Section 3.3.

3.1 Total cross-section

To determine the total cross-section for the production of one or more neutral fragments from electron-impact on LiH_2^-, the rate of fragmentation events observed by the neutral fragment detector has to be related to the total number of electrons and ions present in the interaction region. While the electron density n_e can be deduced from the known current and geometry of the electron beam, the absolute number of ions was too small to be determined by the diagnostic devices of the storage ring. However, as a measure of the number of ions the neutral count rate R_{ref} at the fixed electron energy $E_{ref} = 41.3\,eV$ can be used, which was measured during the *reference* step of the cooler cycle.

To correct for the background due to collisions of LiH_2^- molecules with the residual gas, the rate R_{rg} recorded during the *background* step was subtracted from the rate $R(E_e)$ recorded at the relative energy E_e during the *measurement* step. The rate coefficient α for electron-induced production of neutral fragments is thus given by

$$\alpha(E_e) = \mathcal{N}\,\frac{R(E_e) - R_{rg}}{R_{ref}\;n_e}. \qquad (1)$$

Because of the unknown total number of molecular ions in the storage ring, only the *relative* rate coefficient can be given, that is, $\alpha(E_e)$ is known up to an arbitrary normalization factor $\mathcal{N}$.

The cross-section $\sigma(E_e)$ is connected to $\alpha(E_e)$ through the relation $\alpha(E_e) = \langle\sigma v\rangle$, with the averaging according to the distribution of relative electron velocities v at the given detuning energy E_e. In the present case, where detuning energies of several eV are considered, the effect of electron and ion temperatures is small, and the cross-section σ can be approximated by

$$\sigma(E_e) = \mathcal{N}'\,\frac{\alpha(E_e)}{\sqrt{E_e}}. \qquad (2)$$

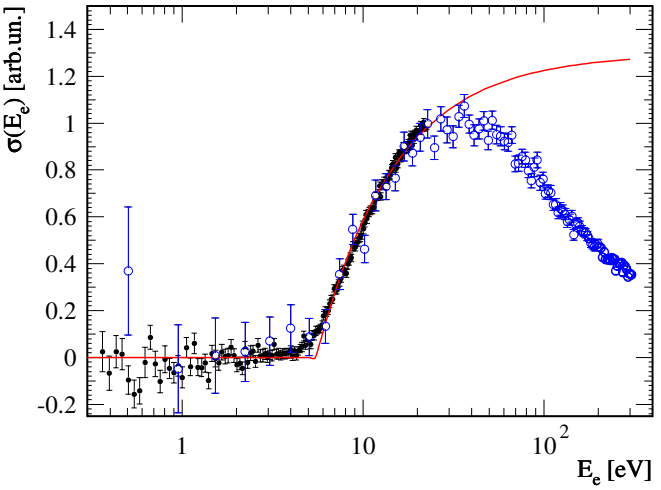

Fig. 3. (Color online) Cross-section σ for the production of at least one neutral fragment by electron impact on LiH_2^- as a function of the electron energy E_e (ion storage time 2–15 s). *Circles*: experimental data (two independent sets of data, with larger statistical errors at low energy for the data shown by open circles), *line*: fit to a classical reaction model (3).

Figure 3 shows the cross-section determined in the present experiment compared to a classical reaction model [15] developed for the description of the electron-impact detachment of electrons from atomic anions. This model assumes a constant probability p for a detachment reaction, given that the electron gets closer to the anion than a reaction radius ρ, which (in atomic units) corresponds to a threshold energy $E_{th} = 1/\rho$. The model thus predicts a cross-section of

$$\sigma(E_e) = \begin{cases} p\pi\rho^2\left(1 - \frac{E_{th}}{E_e}\right) & (E_e > E_{th}) \\ 0 & (E_e \le E_{th}) \end{cases}. \qquad (3)$$

The line in Figure 3 represents a fit of this model to the experimental data in the region $E_e = 0$–$20\,eV$, adjusting the threshold energy E_{th} and an overall normalization factor. Despite the fact that this model is strongly simplifying the situation in a polyatomic molecule, the quality of the fit is comparable with that obtained for atomic [15] and diatomic [16] anions. A threshold energy of $E_{th} = 5.5\,eV$ is found, slightly higher than the detachment energy of 3 eV. This is a common behavior owing to the Coulomb repulsion the incident electron has to overcome to approach the ion close enough for inducing a detachment reaction [15].

The deviation of the reaction model and the experimental data at high energies is expected, as here the assumption of constant reaction probability p is no longer valid. The small deviation in the threshold region can have several reasons, among them quantum effects not covered by the classical model, an anisotropy of the detachment threshold due to the extended geometrical structure of the molecule, vibrational motion, or an experimental artifact stemming from electron-ion collisions at higher energies in the toroid magnets which bend the electron beam into the ion beam orbit (see Fig. 2).

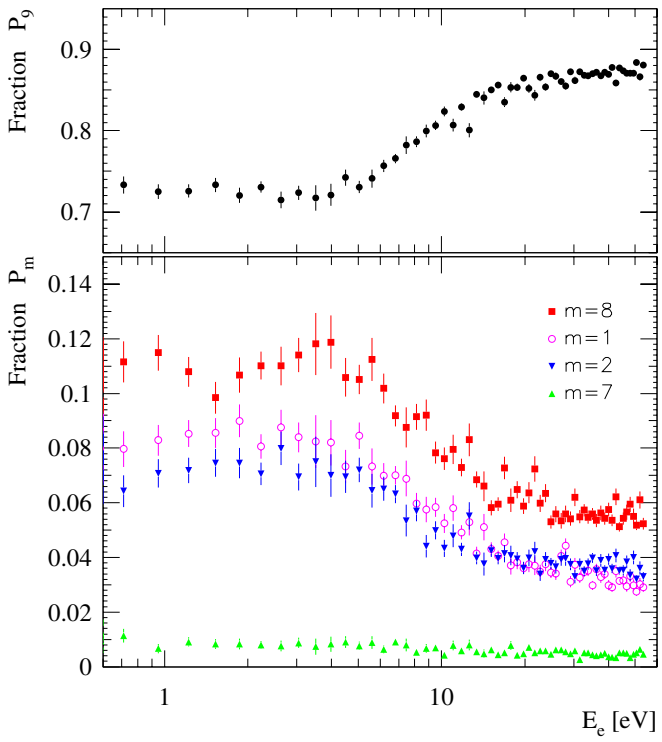

Fig. 4. (Color online) Fraction P_m of events with a total mass $m = 1$, 2, 7, 8, 9 of detected neutral fragments as a function of the electron energy E_e, including also residual gas induced events (ion storage time 2–15 s).

At the given experimental resolution, the two electronic states expected to be accessible by detachment of a valence electron are thus not distinguishable. However, the absence of further steps or resonances in the cross-section suggests that higher PESs do not contribute significantly to the observed fragmentation reaction, and that no intermediate dianions are formed.

3.2 Branching ratios

For a closer inspection of the fragmentation process, the chemical composition of the emerging fragments was investigated. Firstly, the energy resolution of the solid state detector was used to determine the total mass of neutral fragments for each dissociating molecule. Events with a total mass $m < 9$ in particular could be a signature of dissociation events including a charged fragment. When applying relative electron energies above ∼10 eV, the full mass of 9 a.m.u. of the employed $^7LiH_2^-$ ions was observed for a fraction of 90% of all dissociation events (see Fig. 4). This corresponds to the detachment of an electron, possibly followed by a breakup of the neutral system into smaller uncharged fragments. For the remaining 10% of fragmenting molecules a lower total mass was recorded at the neutral fragment detector. Together with the results discussed below, which indicate only a small fraction (on the few-percent level) of non-dissociated neutral products, we conclude [17] that (a) the geometrical detection efficiency of the set-up (see end of Sect. 2) lies at >90% for electron-produced fragments and (b) the possible fraction of dissociation events including a charged fragment is below 10%. In particular, within these limits no evidence for a dissociative excitation through a low-lying excited anion state is found, which can produce both neutral and charged fragments.

For electron energies below ∼10 eV, the fraction of full mass observations drops to 75%. This is consistent with the behavior expected for small geometrical detection losses: residual gas induced fragmentations, which dominate at small electron energies, can be observed also from regions of the storage ring where the ion beam is not accurately pointed to the neutral fragment detector, thus enabling some fragments to geometrically miss the detector. In essence, we find that the large majority of the observed events represent true electron impact detachment yielding only neutral products.

To investigate the chemical composition of fast neutral dissociation fragments, a well established approach (see e.g. [18]) is to reduce the detection efficiency for individual fragments by a known factor by means of inserting metal grids with a geometrical transmission ratio limited through a fine mesh pattern with a fixed spatial period small compared to structures in the spatial fragment distribution. From the observed relative size of the lower-mass peaks in the mass spectrum, indicating events where individual fragments have been absorbed by the grid, it is then often possible to deduce branching ratios for the channels in question. In the present case, the situation was complicated through the large number of channels that had to be considered. Due to the limited a priori knowledge on the breakup process and the significant amount of lower-mass events observed without a grid, all 10 possible combinations of atomic and molecular fragments which can be formed out of up to one lithium and two hydrogen atoms had to be taken into account.

In this situation the usual algebraic derivation of detailed branching ratios from the mass spectrum observed with a grid was not possible. However, by taking advantage of the enlarged set of experimental data obtained by combining the spectra recorded with two grids of different transmission (64% and 27%), and by using the fact that negative branching ratios are unphysical, the general trend of the breakup process could be extracted [17].

The by far dominating channel comprising $\gtrsim$75% of all fragmentation events was found to be the two-body decay into LiH + H (see Fig. 5), while all other channels contributed only few percent each. At the given statistical and systematical uncertainties no evidence for an electron induced reaction through channels different from LiH + H can be concluded.

Since this result is basically independent of the energy of the colliding electron, both electron-induced and residual gas induced dissociation appear to proceeded mostly through the LiH + H channel. In the latter case, as expected, the efficiency for a complete detection of all fragments is reduced, leading to a slight decrease of the observed LiH + H fraction at small ($\lesssim$10 eV) energies.

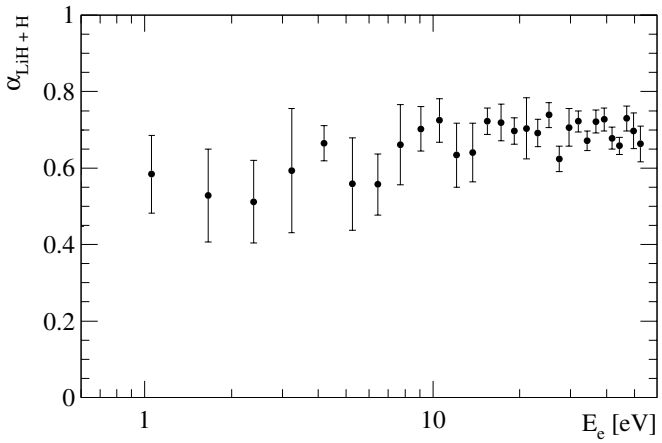

Fig. 5. Branching factor of the LiH + H channel as a function of the electron energy E_e (including residual gas collisions; ion storage time 2–15 s).

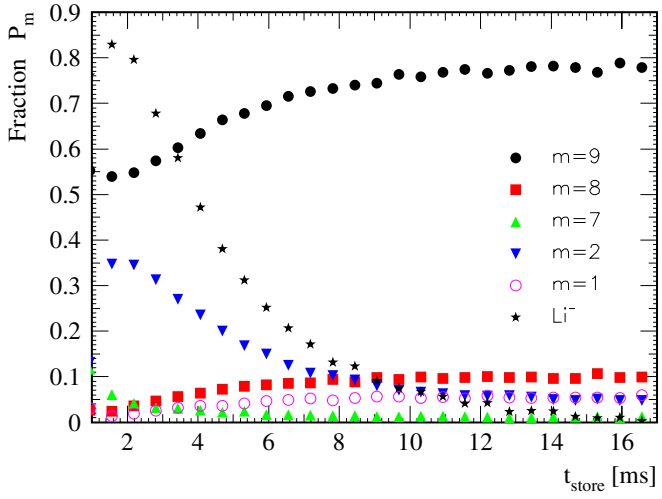

Fig. 6. (Color online) Fraction P_m (relative to the total neutral event rate) of events with a total mass $m = 1$, 2, 7, 8, 9 of detected neutral fragments and of Li^- ions as a function of the storage time t_{store}. The electron energy E_e was fixed to 41.3 eV; residual gas induced events are included.

The results discussed so far were found to be independent of the ion storage time over the observed interval of $t_{store} = 2–15$ s.

3.3 Short time behavior

In the first ms after injection of the molecular ions into the storage ring, also the negative fragment detector revealed a signal, which was due to Li^- ions produced by the stored beam. To shed more light on this observation, the count rates on both the neutral and the negative ion detectors were examined in more detail for these short storage times. Figure 6 shows the fractional contribution of events with different total masses of neutral fragments, observed at $E_e = 41.3$ eV. In addition to the neutral mass fractions

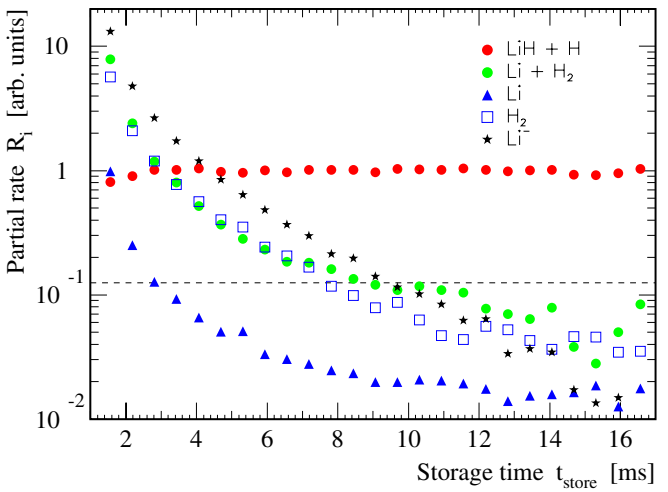

Fig. 7. (Color online) Partial rates of the dominant neutral breakup channels and Li^- rate as a function of the storage time t_{store}. The electron energy was kept at $E_e = 41.3$ eV; residual gas induced events are included. Channels with low contribution are not shown, their individual partial rates would appear below the dashed line.

P_m, the detected rate of Li^- ions is plotted, normalized as all the other rates to the sum of all events involving neutral fragments. The negative ion detector could distinguish between Li^- and LiH^-, however, no LiH^- ions were detected at any storage time. Error bars are omitted here for clarity; the different uncertainties sum up to errors of several percent.

As seen in Figure 6, the neutral mass fractions approach constant values after ~12 ms of storage. Those values are comparable to the fractions observed for storage times of several seconds. In the first few ms after injection, however, the neutral mass fractions significantly differ from this distribution, showing now a strong contribution of $m = 2$ events; also the otherwise very weak $m = 7$ signal is significantly higher at small t_{store}. At the same time, a high rate of Li^- fragments is observed.

To clarify which dissociation channels contribute to the observed neutral mass fractions, the grid method was used also here and branching ratios were determined as a function of storage time. Together with the varying total neutral count rate, these yield the time dependent partial rate R_i for each channel i. Figure 7 shows these partial rates for the dominant neutral channels, together with the observed rate of Li^- ions.

Obviously, the partial rate of the LiH + H channel, which is dominating at long storage times, is basically constant even in the first milliseconds after injection. An additional contribution to the neutral signal at very short storage times comes from the Li + H_2 and H_2 channels. Their count rates are initially up to a factor of 10 higher than for the LiH + H channel, but decrease very rapidly following a roughly exponential decay with a mean lifetime of 2.8 ± 0.1 ms. The same behavior is exhibited by the Li^- ion rate, which strongly suggests that the observed H_2

Table 1. Properties of the observed 'transient' and 'stable' components of the stored LiH_2^- ion beam.

	Transient state	Stable state
Fragmentation channels	$Li + H_2$ and $Li^- + H_2$	$LiH + H$
Observed decay rate Γ ($E_e = 0\,eV$)	$360 \pm 15\,s^{-1}$	$0.63 \pm 0.04\,s^{-1}$ [a)]
transition rate to the stable state	$\lesssim 270\,s^{-1}$	—
fragmentation rate	$\gtrsim 90\,s^{-1}$	$0.63 \pm 0.04\,s^{-1}$ [a)]
Result of electron impact ($E_e = 41.3\,eV$)	none observed	increase of Γ ($\times 4.5$)
Initial population	$\sim$5–25%	$\sim$75–95%

[a)] As deduced from the observed lifetime of the stored beam.

and Li^- fragments originate from the same dissociation channel, namely $LiH_2^- \rightarrow Li^- + H_2$. Remarkably, almost the same decay time of the partial rate is observed not only for H_2 and Li^-, but also for the $Li + H_2$ channel. The channel for which only a Li atom is observed among the neutral products represents the $m = 7$ contribution described before. Its size is compatible with the expected loss of H_2 fragments missing the neutral detector; hence, it does not indicate the occurrence of a further neutral reaction channel.

The experiment thus shows a strong change of the dominant dissociation channel in the first milliseconds of storage, which can only be attributed to changes in the internal state distribution of the molecular ion beam. Apparently, part of the LiH_2^- ions are initially in some *transient* state, dissociating into both the $Li^- + H_2$ and $Li + H_2$ channels with comparable probability.

A similar measurement performed at $E_e = 0\,eV$ yielded essentially the same picture, apart from the reduction of the LiH + H rate expected from the results at long storage times. Thus the decay of the transient anion state seems to be unaffected by electron collisions. Rather, the $LiH + H$ rate attributed to electron interactions seems to be essentially constant in time, while other decay processes occur in addition, unrelated to the presence of electrons. The variation of the $LiH + H$ rate at short times is observed to be <10%, while the rate of channels producing Li^- or Li initially is about 20 times higher than the $LiH + H$ rate. From these numbers it can be derived [17] that at least 25% of the ions stored in the transient state perform fragmentation instead of decaying to the usual, *stable* LiH_2^- state. The numbers are also compatible with fragmentation being the only decay channel of the transient ions. Even if transitions to stable LiH_2^- contribute, the fragmentation rate of the transient ions from these results exceeds $90\,s^{-1}$, which is more than two orders of magnitude larger than the beam loss rate caused by fragmentation of the stable ions. All properties deduced from the measurement in a detailed analysis [17] are summarized in Table 1.

From the present experimental results, no conclusive identification of the nature and decay mechanisms of the observed transient state can be given. However, as discussed below, some tentative explanations of the observed behavior can be given on the basis of theoretically calculated potential energy surfaces (PESs) for the system.

4 Comparison to theory

To clarify the processes underlying the breakup reactions observed experimentally, ab initio calculations using the MOLPRO suite of programs [19] were performed at some selected geometries for the low-lying electronic states of both the neutral LiH_2 and the anionic LiH_2^- system. The internally contracted multi-reference configuration interaction method (MRCI) [20,21] with both single and double excitations of all electrons was employed. Dunnings augmented correlation consistent triple-zeta (AVTZ) basis set [22,23] was chosen for the H-atoms while the standard correlation consistent triple-zeta (VTZ) basis set, augmented by two even tempered SPD functions with ratio 2, was chosen for the Li-atom, leading to 122 primitive and 94 contracted atomic orbitals. The inclusion of diffuse functions for hydrogen and even tempered SPD sets for lithium is crucial for a correct description of the excited states of both the neutral and the anionic system. The CI wave functions are based on the state-averaged complete active space self-consistent field (CASSCF) wave function [24,25] with full-valence active space, leading to 60 and 30 reference configurations for the singlet A' and A'' states of anionic LiH_2^- and 35 and 15 reference configurations for the doublet A' and A'' states of neutral LiH_2, respectively.

To parametrize the three-dimensional space of internal nuclear geometries, the coordinates ϕ, r and x are chosen as follows: ϕ describes the H-Li-H bond angle, while the hyperradius r and the dimensionless symmetry coordinate x are defined by

$$r = \frac{r_1 + r_2}{2} \qquad \text{and} \qquad x = \frac{r_1 - r_2}{r_1 + r_2}\,, \tag{4}$$

with the Li-H bond lengths r_1 and r_2.

To visualize the behavior of the three-dimensional PESs, two-dimensional cuts of the coordinate space are defined by setting one of the hyperangles x or ϕ to a fixed value. The potential energy is then plotted as a function of the second hyperangle with the hyperradius r *optimized* for minimum energy at each point (separately for each plotted PES). In particular, two such cuts are discussed, which describe the transition from the LiH_2^- equilibrium geometry to the geometries of the two asymptotic channels which were observed in the experiment, namely $LiH + H$ and $Li + H_2$.

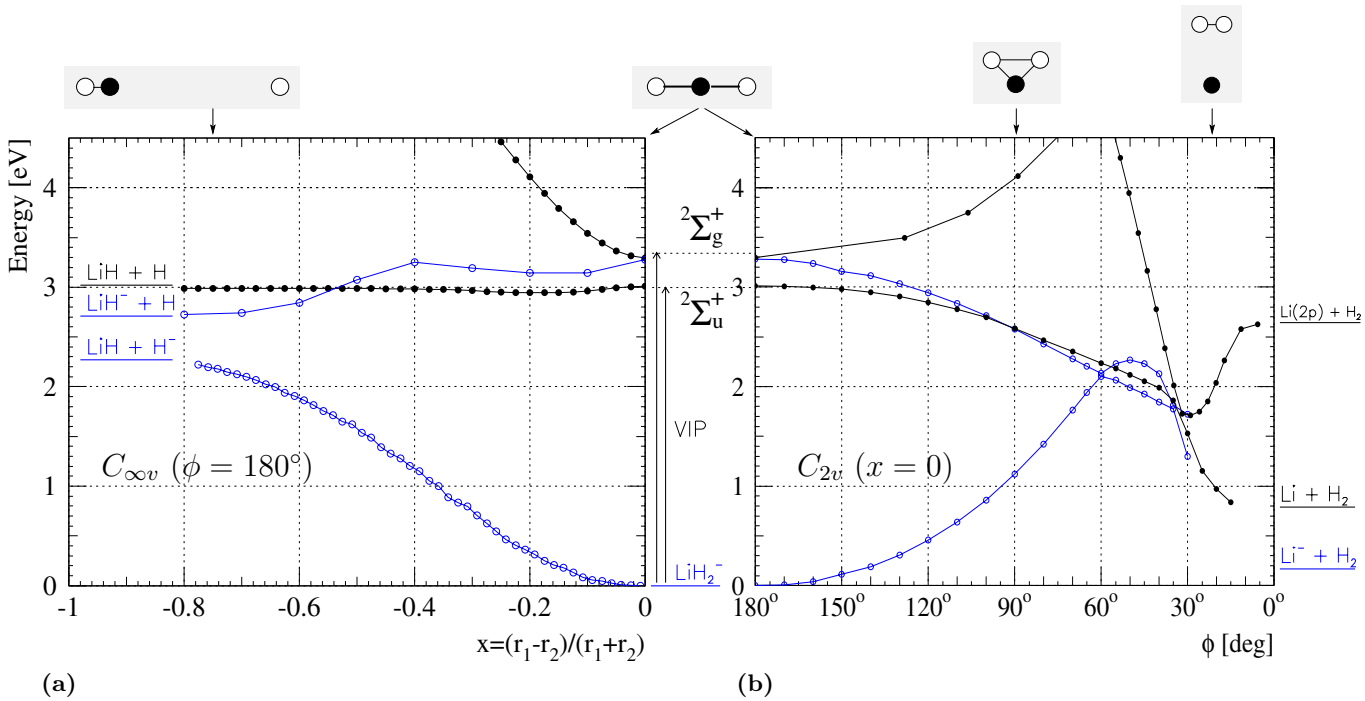

Fig. 8. (Color online) Calculated potential energy surfaces for the neutral LiH_2 (full circles) and the anionic LiH_2^- system (open circles). Energies of the two lowest states are given (a) as a function of x, with ϕ set to 180° ($C_{\infty v}$ symmetry) (b) as a function of ϕ, with x set to 0 (C_{2v} symmetry). The hyperradius r was optimized for minimum energy at each point. The geometry of the system is indicated by the pictograms.

Figure 8a shows the transition from the LiH_2^- configuration ($x = 0$) to the LiH + H asymptote ($x \to \pm 1$) along linear geometries ($\phi \equiv 180°$). In Figure 8b the transition to the Li + H_2 asymptote through a closing of the H-Li-H bond angle ϕ is shown, restricted to isoceles geometries ($x \equiv 0$). Energies of the asymptotic channels and the LiH_2^- Vertical Ionization Potentials are indicated, as taken from Figure 1 after correction for zero-point energies.

In view of these calculated PESs, the dominance of the LiH + H channel observed at long storage times seems to be rather surprising. After a vertical transition to the lowest PES of the neutral system (labeled $^2\Sigma_u^+$ at the $D_{\infty h}$ geometry of the anion), this channel is here found energetically open by only ∼20 meV. While corrections due to vibrational zero-point oscillations of the molecular species involved could slightly increase this value, a propagation of the neutral system towards the Li($2s$) + H_2 channel, with an energy release of more than 2 eV, appears to be much more likely. In addition, the pathway to LiH + H was found to be unstable vs. distortions of the $C_{\infty v}$ symmetry, while the path to Li + H_2 along the C_{2v} symmetry follows a minimum of the PES with respect to distortions of this symmetry.

However, a first step towards explaining the experimental findings could be made by taking into account the second neutral state $^2\Sigma_g^+$. The shape of this PES is similar to the anionic ground state; thus the favorable Franck-Condon overlap should strongly enhance detachment reactions populating this state once the colliding electron has sufficient energy. This excited state will then undergo a rapid radiationless transition to the neutral ground state, accompanied by a transfer of energy from electronic to vibrational degrees of freedom. The detailed processes governing the transitions between these three PESs and in particular the interplay of electronic and vibrational energy might bear the physical reason for a initial propagation of the system in the direction of the LiH + H geometry following electron detachment. However, with such a mechanism alone one still cannot explain why the system indeed reaches the LiH + H asymptote in spite of the noted instability of the pathway vs. perturbations of the linear shape. Hence, the observation of this pathway as the dominant one opens up a number of interesting unsolved questions regarding the underlying reaction dynamics.

Another open question is the nature of the transient state of the anion observed experimentally at short storage times, which decays mainly into $Li^- + H_2$ and Li + H_2 (corresponding to the geometries in Fig. 8b). In principle, this state could differ from the usual, stable LiH_2^- state in three ways: it could either exhibit an exceptional vibrational excitation or an alternative geometry corresponding to a displaced, local minimum of the electronic ground state PES, or it might belong to another, excited PES.

To enable a dissociation of the system by tunneling through the potential barrier at $\phi = 60°$ from a vibrationally excited state, a very high excitation level ($v \gtrsim 38$) of the bending mode would be required [17]. A high vibrational excitation level at the same time would be accompanied by a significant population of moderately excited levels which cannot dissociate by tunneling. Due to their

geometry, these excited ions would however be expected to fragment after *electron detachment* significantly to the $Li + H_2$ channel. However, such an *electron induced* contribution to the $Li + H_2$ signal at short storage times is not observed experimentally (see Sect. 3.3). This makes the existence of a high initial bending mode excitation of the stored LiH_2^- ions unlikely.

As a second candidate, the electrostatic complex configuration $Li^-(H_2)$ found in recent ab initio calculations [4] has to be considered. The geometry of this complex is close to the $Li^- + H_2$ asymptote with an equilibrium distance of 11.6 a.u. between the Li^- ion and the center of the electrostatically attached H_2 molecule. The complex is very weakly bound, the adiabatic dissociation energy D_0 with respect to the $Li^- + H_2$ asymptote being only 0.9 meV (2.7 meV) for the para (ortho) nuclear spin configuration of the H_2 molecule [4]. Such a state, if produced in the ion source, would be dissociated by interactions with the surrounding 300 K blackbody radiation, with the observed lifetime of ∼3 ms being of reasonable order of magnitude. On the other hand, the experiment shows a considerable flux also towards the neutral $Li + H_2$ channel. Here an additional energy of 0.62 eV is required for detachment of an electron; therefore an identification of the observed transient state as the electrostatic complex would contradict the finding of equal rates at the neutral and anionic fragmentation channels.

The third option to be considered here is a metastable state belonging to an electronically excited PES of the anion. This would require a local minimum of an excited PES at a geometry that allows for the breakup into $Li + H_2$ as well as $Li^- + H_2$. The energy of this state should be below that of the neutral system to avoid a rapid autodetachment inhibiting the fragmentation into $Li^- + H_2$.

A good candidate for such a situation might be the conical intersection of the two lowest electronic states of the anion which appears at the geometry of an equilateral triangle ($\phi = 60°$, $x = 0$). Because of the strong coupling at the intersection point, a vibrational ground state wave function supported by the conically shaped minimum of the upper PES would be expected to decay very fast by transitions to the lower surface, probably much faster than the lifetime observed. However, a vibrationally excited state would exhibit a much lower probability density at this geometry, which might yield the observed lifetime of the transient state of ∼3 ms.

Transitions from the upper to the lower sheet of the PES near the conical intersection should be followed either by an opening of the bond angle and fast vibrational relaxation to the anionic ground state configuration, or by separation of an H_2 molecule. In the latter case the system would pass through a second intersection of the two anionic PESs at $\phi \approx 35°$, a geometry where also the two lowest neutral PESs are energetically very close. Thus, the transition to a neutral PES by autodetachment of an electron appears well possible, in agreement with the observation that the $Li + H_2$ and $Li^- + H_2$ channels occur with comparable yields in the decay of the transient state.

5 Conclusions

While a number of questions have to be left open in this discussion, the present storage ring experiments reveal new and unexpected results when discussed together with theoretical calculations of the properties of the LiH_2^- anion.

Following a transient decay behavior during the first few (∼10) ms, LiH_2^- ions from a cesium sputter ion source show a fragmentation pattern with time-independent properties at >20 ms storage time. The electron-induced fragmentation of LiH_2^- is dominated by the detachment of an electron and the subsequent dissociation into the neutral LiH + H channel. The fragmentation towards this channel proceeds in the geometrically unstable electronic ground state of the neutral system, but the first excited neutral state is likely to play an important role as an intermediate state directly following the electron detachment. The strong dominance of the LiH + H channel over the $Li + H_2$ channel, clearly observed in the experiment, is unexpected in view of the potential energy landscape, and needs further theoretical consideration. A breakup into a channel containing a negative fragment via dissociative excitation was not observed.

The second and just as much unexpected result is the finding of a transient state of the anion with a lifetime of 2.8 ms and an estimated population of ∼5–25% at the time of production of the molecular ions in the sputter ion source. This state was found to decay rapidly, and basically independent of electron impact, by fragmentation into both the $Li + H_2$ and $Li^- + H_2$ channels at equal rate.

The nature of this state could not be derived conclusively on the basis of available theoretical knowledge. More detailed theoretical calculations are desirable here to study the properties of potential candidate systems, such as highly vibrationally excited or electronically metastable states. On the experimental side, studies of the short-time behavior under variable environmental conditions, such as different residual gas pressure or surrounding temperature might help to clarify the origin of this transient decay.

This work has been funded in part by the German-Israeli Foundation for Scientific Research (GIF) under contract I-707-55.7/2001.

References

1. A.I. Boldyrev, J. Simons, J. Chem. Phys. **99**, 4628 (1993)
2. J. Senekowitsch, P. Rosmus, J. Chem. Phys. **86**, 6329 (1987)
3. S.B. Sharp, G.I. Gellene, J. Chem. Phys. **113**, 6122 (2000)
4. D.T. Chang, G. Suttatt, G. Ristroff, G.I. Gellene, J. Chem. Phys. **116**, 9188 (2002)
5. E. Heinicke, K. Bethge, H. Baumann, Nucl. Instr. Meth. **58**, 125 (1968)
6. H.W. Sarkas, J.H. Hendricks, S.T. Arnold, K.H. Bowen, J. Chem. Phys. **100**, 1884 (1993)
7. P.C. Stancil, S. Lepp, A. Dalgarno, Astrophys. J. **458**, 401 (1996)

8. J.-J. Chen, K.-C. Lin, J. Chem. Phys. **119**, 8785 (2003)
9. H.S. Lee, Y.S. Lee, G.-H. Jeung, J. Phys. Chem. A **103**, 11080 (1999)
10. K.H. Kim, Y.S. Lee, T. Ishida, G.-H. Jeung, J. Chem. Phys. **119**, 4689 (2003)
11. W.C. Stwalley, W.-T. Zemke, J. Phys. Chem. Ref. Data **22**, 87 (1993)
12. E.E. Eyler, N. Melikechi, Phys. Rev. A **48**, R18 (1993)
13. T. Andersen, H.K. Haugen, H. Hotop, J. Phys. Chem. Ref. Data **28**, 1511 (1999)
14. D. Habs et al., Nucl. Instr. Meth. B **43**, 390 (1989)
15. L. Vejby-Christensen, D. Kella, D. Mathur, H.B. Pedersen, H.T. Schmidt, L.H. Andersen, Phys. Rev. A **53**, 2371 (1996)
16. H.B. Pedersen, N. Djuric, M.J. Jensen, D. Kella, C.P. Safvan, H.T. Schmidt, L. Vejby-Christensen, L.H. Andersen, Phys. Rev. A **60**, 2882 (1999)
17. L. Lammich, Ph.D. thesis, University of Heidelberg, 2004
18. L. Vejby-Christensen, L.H. Andersen, O. Heber, D. Kella, H.B. Pedersen, H.T. Schmidt, D. Zajfman, Astrophys. J. **483**, 531 (1997)
19. `MOLPRO`, *a package of ab initio programs designed by H.J. Werner, P.J. Knowles, version 2002.1*, R.D. Amos et al.
20. H.-J. Werner, P.J. Knowles, J. Chem. Phys. **89**, 5803 (1988)
21. P.J. Knowles, H.-J. Werner, Chem. Phys. Lett. **145**, 514 (1988)
22. T.H. Dunning Jr, J. Chem. Phys. **90**, 1007 (1989)
23. R.A. Kendall, T.H. Dunning Jr, R.J. Harrison, J. Chem. Phys. **96**, 6796 (1992)
24. H.-J. Werner, P.J. Knowles, J. Chem. Phys. **82**, 5053 (1985)
25. P.J. Knowles, H.-J. Werner, Chem. Phys. Lett. **115**, 259 (1985)